Censored Spatial Wind Power Prediction with random effects

Carsten Croonenbroeck

Daniel Ambach

European University Viadrina Frankfurt (Oder)

Department of Business Administration and Economics

Discussion Paper No. 362

November 2014

ISSN 1860 0921

Censored Spatial Wind Power Prediction with Random Effects

November 4, 2014

Carsten Croonenbroeck[a] and Daniel Ambach[b]

Abstract

We investigate the importance of taking the spatial interaction of turbines inside a wind park into account. This article provides two tests that check for wake effects and thus, take spatial interdependence into account. Those effects are suspected to have a negative influence on wind power production. Thereafter, we introduce a new modeling approach that is based on the Generalized Wind Power Prediction Tool (GWPPT) and therefore respects both-sided censoring of the data. Furthermore, the new model takes a Spatial Lag Model (SLM) specification into account and allows for random effects in the panel data. Finally, we provide a short empirical study that compares the forecasting accuracy of our model to the established models WPPT, GWPPT, and the naïve persistence predictor. We show that our new model provides significantly better forecasts than the established models.

JEL classification: C31, C34, E27, Q47
Keywords: Spatial Lag Model, Censored, Regression, Wind Power, Forecasting, Random Effects

Addresses:

[a] Corresponding Author: Carsten Croonenbroeck, European University Viadrina, Chair of Economics and Economic Theory (Macroeconomics), Post Box 1786, 15207 Frankfurt (Oder), Germany, Tel. +49 (0)335 5534 2701, Fax +49 (0)335 5534 72701, E-Mail: croonenbroeck@europa-uni.de.

[b] Daniel Ambach, European University Viadrina, Chair of Quantitative Methods and Statistics, Post Box 1786, 15207 Frankfurt (Oder), Germany, Tel. +49 (0)335 5534 2983, Fax +49 (0)335 5534 2233, E-Mail: ambach@europa-uni.de.

Censored Spatial Wind Power Prediction with Random Effects

November 4, 2014

Abstract

We investigate the importance of taking the spatial interaction of turbines inside a wind park into account. This article provides two tests that check for wake effects and thus, take spatial interdependence into account. Those effects are suspected to have a negative influence on wind power production. Thereafter, we introduce a new modeling approach that is based on the Generalized Wind Power Prediction Tool (GWPPT) and therefore respects both-sided censoring of the data. Furthermore, the new model takes a Spatial Lag Model (SLM) specification into account and allows for random effects in the panel data. Finally, we provide a short empirical study that compares the forecasting accuracy of our model to the established models WPPT, GWPPT, and the naïve persistence predictor. We show that our new model provides significantly better forecasts than the established models.

JEL classification: C31, C34, E27, Q47
Keywords: Spatial Lag Model, Censored, Regression, Wind Power, Forecasting, Random Effects

1 Introduction

Research on wind power forecasting has been manifold in recent years. Lei et al. (2009) as well as Giebel et al. (2011) provide a brief overview of the wide range of model types, whether they may focus on wind speed forecasting or on wind power forecasting directly. Models may approach the problem of wind power forecasting from different perspectives. There are physics based, engineering, meteorological or statistical approaches. Engineering models utilize machine learning algorithms, for instance, Artificial Neural Networks (ANNs) or Support Vector Machines (SVMs). Stochastic models may be based on univariate time series approaches like periodic autoregressive moving average processes (ARMA). One state-of-the-art model for wind power predictions is the Generalized Wind Power Prediction Tool (GWPPT), as introduced by Croonenbroeck and Dahl (2014). GWPPT is the generalization of the Wind Power Prediction Tool (WPPT) by Nielsen et al. (2007), which has come to broad worldwide usage. While WPPT is based on a linear estimation of the relationship between wind speed and wind power (Power Curve) and a diurnal Fourier Series, GWPPT additionally takes wind direction into account and also considers the non-linearity of the Power Curve by using a both-sided censored estimation procedure.

However, most models do not exploit the spatial distribution of their target turbines. Alexiadis et al. (1999) provide early work on spatial analysis and use an ANN to obtain both wind speed and wind power forecasts. Damousis et al. (2004) combine spatial modeling with a genetic algorithm to fit and predict their data. More recently, Han and Chang (2010) use a simulation study to analyze the impact of spatial and time correlation on wind power forecasting accuracy. Hering and Genton (2010) as well as Xie et al. (2011) cover the spatial dependence structure by regime switching models. Following these research contributions, Díaz et al. (2014) sum up the importance of taking the spatial composition of wind parks into account. They state: "In clusters of wind generators spread over small geographic areas, the spatial correlation of wind power production is strong."

Forecasting wind power for several turbines located in one wind park may benefit from the exploitation of the spatial arrangement of the turbines. Clearly, if two turbines are in a row (given the respective wind direction), there should be some interaction. Here, we have to consider wake effects, as discussed by Kim et al. (2015). Therefore, we observe that the wind direction has a local influence on the wind speed at the turbines in a wind park. Furthermore, spatial correlation is very much likely. Taking it into consideration may be of avail for

forecasting models.
In this article, we first introduce several straight-forward test approaches for empirical wake effect analysis. That provided, we base our forecasting model on GWPPT, but introduce a spatial generalization of it that also takes random effects into account. We show that our new model is capable of improving out-of-sample forecasting accuracy by a severe degree over the plain GWPPT model.
The article is structured as follows. Section 2 presents the data structure and investigates properties of the actual observed wind park. In Section 3 we introduce the model and discuss its in-sample performance and properties. Section 4 sheds light on out-of-sample results and Section 5 concludes.

2 Description and analysis of the data set

The wind power data set used in this article is a high-frequency series collected in Germany. It consists of four different Fuhrländer FL MD 77 turbines located at one wind park. The observed wind park is situated in a rural plain region. The area has a slight roughness with fields and some forests. Due to a non-disclosure agreement, the specific locations cannot be revealed. However, Figure 1 presents a stylized map of the turbine's arrangement. The turbines, labeled Turbine A to D, exhibit a power range of each $[0; 1500]$ kW and write sensor data to log files at a frequency of ten minutes. The observed time frame spans from November 1, 2010 to November 5, 2012, so there are 105984 observations per turbine.

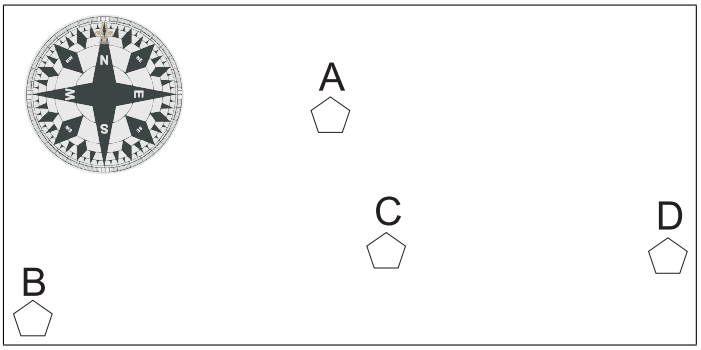

Figure 1. Stylized map of the wind park investigated.

The four turbines represent the individuals in our panel data structure. Therefore, the balanced panel consists of $i = 1, \ldots, n; n = 4$ individuals (turbines), each containing $t = 1, \ldots, T; T = 105984$ observations, which yields

$nT = N = 423936$ observations in total. Table 1 shows descriptive statistics of the data set.

	Wind speed	Power	Azimuth
Minimum	0.4	-19.0	2
First quantile	3.4	0.0	117
Median	5.1	124.0	209
Mean	5.2	224.9	189
Third quantile	6.7	323.7	252
Maximum	19.3	1542.0	357
Variance	6.1	81050.3	6890.3
Skewness	0.5	1.8	-0.4
Kurtosis	3.5	6.6	2.1

Table 1. Descriptive table of the data set. Wind speed denoted in m/s, Power in kW, Azimuth in degrees, 0° = north, clockwise.

Spatial dependencies inside a wind park are expected to be caused by wake induced turbulence effects. Wind wakes are created by upwind turbines and influence downwind turbines. As wind direction determines which turbines are upwind or downwind, the direction itself has a direct impact on the wind power production. As wake effects subside with increasing distances, we expect that turbines at rather short distances (as it is usual in typical wind parks) have a strong impact on each other. However, as Kim et al. (2015) point out, this should hold true only for wind speeds above cut-in speed and below the region of rated output (see Figure 2).

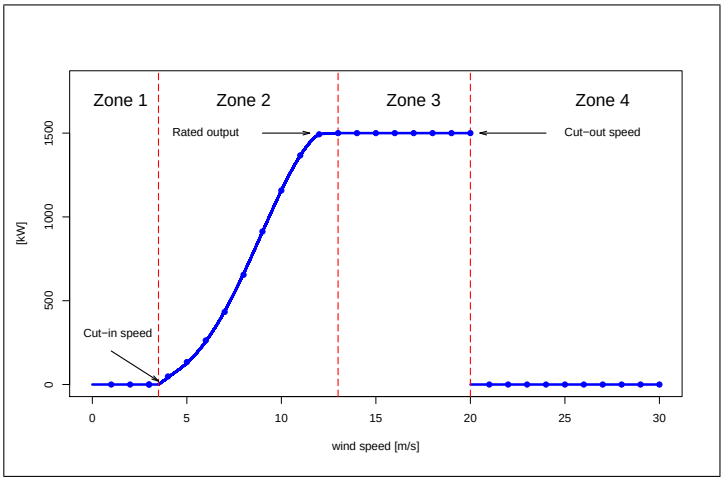

Figure 2. Power function of the Fuhrländer FL MD 77.

Thus, if the wind speed reaches a certain zone, we observe either no spatial dependency (Zones 1 and 3) or we expect a dependency structure (Zone 2). For the latter case, we observe that the wind speed and the wind direction influence the wind power. However, there is no spatial dependence if the wind speed is below cut-in speed and the turbines do not work. The same holds in the rated output zone. Here, the wind can push the turbine to its maximum power load, even if turbulence is present. This hypothesis can be formulated by means of conditional expectations.

Hypothesis 1. *We observe two turbines, where Turbine 1 is an upwind turbine and Turbine 2 is a downwind one. If the wind speed is in Zone 2 (see Figure 2), we expect wake effects and as such, the wind power production at Turbine 1 should be significantly larger than that of Turbine 2. Formally, that test can be described as*

$$\mathbb{E}\left[\mathcal{P}_1 - \mathcal{P}_2 \middle| \mathcal{A}_1 \in \left[\mathcal{A}_1^l, \mathcal{A}_1^u\right], \mathcal{W}_1 \in \left[\mathcal{W}_1^l, \mathcal{W}_1^u\right]\right] > 0, \tag{1}$$

where $\mathcal{P}_i$ is the power production of Turbine i, $\mathcal{A}_i$ is the wind direction at Turbine i, and $\mathcal{W}_i$ is the wind speed at Turbine i. Furthermore, $\mathcal{A}_i^l$ is the lower bound of an interval of wind directions, $\mathcal{A}_i^u$ is the respective upper bound, and $\mathcal{W}_i^l$ and $\mathcal{W}_i^u$ are the respective bounds of an interval of wind speeds.

For example, Turbine C is almost exactly in the wake of Turbine D, provided wind directions from the east. For this case, a wind directions interval is chosen to be $\mathcal{A}_D \in [80, 100]$. Choosing a relevant wind speed interval, say, $\mathcal{W}_D \in [5, 8]$, the test can be carried out by calculating the conditional mean and applying a simple t-Test. The aforementioned interval is within Zone 2 and therefore we expect a spatial dependence.
As an alternative, a test can aim directly at the perceived wind speeds at the turbine located inside the wake of another turbine.

Hypothesis 2. *Provided that Turbine 2 is a downwind turbine and Turbine 1 is an upwind turbine, the measured wind speed at Turbine 1 should be significantly larger than that of Turbine 2. Formally, that test can be described as*

$$\mathbb{E}\left[\mathcal{W}_1 - \mathcal{W}_2 \middle| \mathcal{A}_1 \in \left[\mathcal{A}_1^l, \mathcal{A}_1^u\right]\right] > 0. \tag{2}$$

Turbine 1	Turbine 2	Wind speed	Wind direction	Test value - Hyp. 1	Test value - Hyp. 2
Panel A					
D	C	[5, 8]	[80, 100]	***61.1624	***0.2835
B	A	[5, 8]	[215, 235]	***57.2533	***0.4138
C	A	[5, 8]	[160, 180]	***73.7584	***0.3490
Panel B					
C	D	[5, 8]	[170, 190]	12.7457	0.0192
A	D	[5, 8]	[225, 225]	8.9184	0.0927
B	D	[5, 8]	[335, 355]	8.1284	*0.1117
Panel C					
D	C	[0, 3]	[80, 100]	0.4581	0.0018
D	C	[14, 19]	[80, 100]	*89.5643	*1.0619

Table 2. Several outcomes for empirical tests hypothesis 1 and 2. ***, ** and * represent significance at 1%, 5%, and 10% level.

For our wind park, many constellations are possible. Table 2 provides a few examples. It presents test values for the selected turbine, the wind speed, the wind direction and the test values for hypotheses 1 and 2. In Panel A, we consider combinations of turbines where wake effects are present. Panel B shows results for constellations at which Turbine 1 is not upwind of Turbine 2. Panel C finally contains cross check values at which wake effects are possible, but wind speeds are too low or too high. Test results for Panel A are significant. Concerning Panels B and C, the test results are mostly insignificant. After all, we conclude that the spatial structure is important. Therefore, we construct a model that exploits the spatial interdependency for the in-sample fit and out-of-sample forecasting.

3 Model description and its in-sample properties

As a first approach, we exploit the panel structure of our data set by using classical panel estimation procedures. That is, we extend the GWPPT specification for a panel notation:

$$\begin{aligned}\hat{x}_{i,t+k} = m + \alpha_1 \cdot x_{i,t} + \alpha_2 \cdot x_{i,t-1} + b_1 \cdot w_{i,t+k|t} + b_2 \cdot w^2_{i,t+k|t} + \delta \cdot a_{i,t+k} \\ + d^c_1 \cdot \cos\left(\frac{2\pi d_{t+k}}{144}\right) + d^c_2 \cdot \cos\left(\frac{4\pi d_{t+k}}{144}\right) \\ + d^s_1 \cdot \sin\left(\frac{2\pi d_{t+k}}{144}\right) + d^s_2 \cdot \sin\left(\frac{4\pi d_{t+k}}{144}\right) + \varepsilon_{i,t+k}, \quad (3)\end{aligned}$$

where $x_{i,t}$ is the power production of Turbine i at time t, $w_{i,t+k|t}$ is the wind speed at time $t+k$ given time t, $a_{i,t}$ is the wind direction[1], and d_t is the time of the day for observation t. $\varepsilon_{i,t} = \theta_i + \xi_t + \omega_{i,t}$, where θ_i denotes the individual effects, ξ_t denotes the time effects, and $\omega_{i,t}$ is assumed to be Gaussian noise.
Fuhrländer FL MD 77 Turbines are designed to operate at a maximum load of 1500 kW, so it can be assumed that any forecast that lies outside of an interval of $[0; 1500]$ is wrong. GWPPT makes use of this a-priori known information. The model imposes the following structure on wind power:

$$x^*_{i,t} = \eta(\mathbf{z}_{i,t}) + \varepsilon_{i,t}, \tag{4}$$

where $\mathbf{z}_{i,t}$ is the vector of explanatory variables, η is a linear function of $\mathbf{z}_{i,t}$, and $\varepsilon_{i,t}$ satisfies the assumptions above. GWPPT imposes a censored data structure, such that

$$x_{i,t} = \begin{cases} l, & x^*_{i,t} \leq l \\ x^*_{i,t}, & x^*_{i,t} \in (l,u) \\ u, & x^*_{i,t} \geq u, \end{cases} \tag{5}$$

where l and u are the lower and upper censoring points. Parameters are estimated using a generalized Tobit model. In the end, due to assumed Gaussian errors, the forecast is calculated by

$$\hat{x}_{i,t+k} = (\Phi(f_2) - \Phi(f_1)) \cdot x^*_{i,t+k} + (\phi(f_1) - \phi(f_2)) \cdot \widehat{\sigma} + u \cdot (1 - \Phi(f_2)), \tag{6}$$

where

$$f_1 = \frac{l - x^*_{i,t+k}}{\widehat{\sigma}}, \tag{7}$$

$$f_2 = \frac{u - x^*_{i,t+k}}{\widehat{\sigma}}, \tag{8}$$

and $\phi(\cdot)$ and $\Phi(\cdot)$ denote normal PDF (Probability Density Function) and CDF (Cumulative Distribution Function), respectively.
Primarily, we use the classical linear panel estimation and therefore, the usual pooled vs. panel tests are performed. Hence, we calculate the test for unobserved heterogeneity, i.e., the Breusch-Pagan-Lagrange-Multiplier test. If the pooled assumption is rejected, a test for random effects vs. fixed effects, i.e. the Hausman test, is applied. From a theoretical point of view, we prefer a random effects model instead of a fixed effects model for two reasons:

[1]Note that for WPPT, $\delta = 0$.

Conjecture 1. *Fixed effects models assume unobserved heterogeneity to vary over individuals (here: Turbines), but to be constant across time for each individual. We do not assume this to be the case here. Unobserved (or: unobservable) factors may be different wearout for different turbines, different local weather conditions, unconsidered periodicity structure or weather-dependent conditions not accounted for in the underlying WPPT model, such as, e.g., air pressure. None of these factors can be assumed to be constant over time, at least not for time periods longer than "very short" ones.*

Conjecture 2. *Random effects estimators are more efficient, given regressors are strictly exogenous. The regressors in our model are wind speed, wind direction and time. It would be absurd to consider any of those be influenced by wind power itself, the regressand. Thus, exogeneity can safely be assumed.*

Empirically, we reject the hypothesis of a pooled structure ($p \leq 0.0001$) and decide for random instead of fixed effects ($p = 0.6457$). Additionally, we check for spatial autocorrelation using the standard Moran's I test as discussed by Li et al. (2007). The null hypothesis of no spatial autocorrelation is clearly rejected ($p = 0.0079$). Consequently, the encouraging spatial and panel test results guide us to use a spatial model. Thus, we motivate the Spatial Lag Model (SLM):[2]

$$\begin{aligned}\hat{x}_{i,t+k} = \lambda \sum_{j=1}^{N} \varpi_{i,j}\hat{x}_{j,t+k} + \alpha_1 \cdot x_{i,t} + \alpha_2 \cdot x_{i,t-1} + b_1 \cdot w_{i,t+k|t} + b_2 \cdot w_{i,t+k|t}^2 + \delta \cdot A_{i,t+k} \\ + d_1^c \cdot \cos\left(\frac{2\pi d_{t+k}}{144}\right) + d_2^c \cdot \cos\left(\frac{4\pi d_{t+k}}{144}\right) \\ + d_1^s \cdot \sin\left(\frac{2\pi d_{t+k}}{144}\right) + d_2^s \cdot \sin\left(\frac{4\pi d_{t+k}}{144}\right) + \varepsilon_{i,t+k}, \quad (9)\end{aligned}$$

where λ denotes the interaction term and $\varpi_{i,j}$ is the i, j^{th} element of a nonnegative, $N \times N$-dimensional weighting matrix W. As the panel structure is balanced, we generate the weighting matrix by defining a symmetric n-dimensional inverse distance matrix Ω containing the interconnected reciprocal distances of the Turbines[3] and then Kronecker-multiplying it by a T-dimensional matrix of ones, i.e.

[2] We also check several Spatial Error Model (SEM) and Spatial Durbin Model (SDM) specifications, but the tests described by Elhorst (2010) guide us to use SLM modeling.
[3] For some further applications, that matrix should also be row-normalized.

$$W = \Omega \bigotimes \iota_T \iota_T', \tag{10}$$

where ι_T is a T-dimensional column vector of ones. The empirical distance matrix Ω for our wind park is

$$\Omega = \begin{pmatrix} 0 & \frac{1}{118} & \frac{1}{48} & \frac{1}{121} \\ \frac{1}{118} & 0 & \frac{1}{119} & \frac{1}{211} \\ \frac{1}{48} & \frac{1}{119} & 0 & \frac{1}{93} \\ \frac{1}{121} & \frac{1}{211} & \frac{1}{93} & 0 \end{pmatrix}. \tag{11}$$

For the censored random effects estimation procedure, we apply the maximum likelihood approach as described by Henningsen (2010):

$$L_i = \int_{-\infty}^{\infty} \left(\prod_{t=1}^{T_i} \left(\Phi \left(\frac{l - x_{it}^T \beta - \theta_i}{\sigma_\omega} \right) \right)^{I_{it}^l} \left(\Phi \left(\frac{x_{it}^T \beta + \theta_i - u}{\sigma_\omega} \right) \right)^{I_{it}^u} \right.$$
$$\left. \left(\frac{1}{\sigma_\omega} \phi \left(\frac{y_{it} - x_{it}^T \beta - \theta_i}{\sigma_\omega} \right) \right)^{\left(1 - I_{it}^l - I_{it}^u\right)} \right) \phi \left(\frac{\theta_i}{\sigma_\theta} \right) d\theta_i, \tag{12}$$

where β is the vector of parameters. Furthermore, the log-likelihood is given by $\log L = \sum_{i=1}^{N} \log L_i$. The appendix shows the Gauss-Hermite quadrature to solve the integral of the likelihood function.

Table 3 presents the estimation results. All estimates show the expected sign. Three of four Fourier coefficients are insignificant, but this is quite usual in the estimates. The terms represent the diurnal periodicity as introduced for the plain WPPT. The interaction term λ shows a negative sign, representing that the smaller the reciprocal distance (or: the greater the distance) between a pair of Turbines, the greater the power production. In other words, increasing distance leads to decreasing negative influence like wake effects or other spatial dependency impacts.

Coefficient	Estimate
α_1	***1.7345
α_2	***1.1635
b_1	***43.8164
b_2	***22.5735
δ	***–0.0315
d_1^c	**9.1893
d_2^c	3.6844
d_1^s	1.3466
d_2^s	2.3454
λ	***–7.3623
pseudo-R^2	0.9624

Table 3. Estimation results of the censored spatial random effects model. Dependent variable: Wind power. ***, ** and * represent significance at 1%, 5%, and 10% level.

4 Out-of-sample results

Giebel et al. (2011) suggest to use standardized Root Mean Squared Errors (sRMSE) for the comparison of wind power forecasts. The sRMSE is derived by standardizing the RMSE to the basis of the turbine's maximum power output. Thereby, sRMSE values can be compared across several types of Turbines as well as throughout entire wind parks.

For our comparison study, out-of-sample forecasts are calculated. Initially, roughly 60% of the entire time frame (approximately 60000 observations per Turbine) are used as training data. The considered high frequency observations for the in-sample model calibration start from November 1, 2010 and reach to December 7, 2011. Subsequently, we calculate forecasts for 1000 randomly selected observations in the out-of-sample time frame for forecasting horizons of up to 36 hours, which are 216 steps ahead.

The spatial GWPPT model (spGWPPT) derived here is compared to GWPPT, WPPT and the naïve forecast. The naïve model $\hat{x}_{t+k} = x_t$ is a common benchmark in the literature (see, e.g., Costa et al., 2008, or Giebel et al., 2011). Figure 3 presents sRMSE values for Turbine A, for all models and forecasting horizons. While all models, even the primitive persistence model, show low values of sRMSE in short term forecasting horizons, the naïve forecast is clearly outperformed by WPPT at forecasting horizons of 36 steps (6 hours) and longer. However, GWPPT outperforms WPPT significantly. GWPPT shows an interesting behavior. Around 144 steps ahead (24 hours), sRMSE decreases. This

can be explained by diurnal periodicity: At daily periods, it may be that the forecaster actually returns better forecasts than at shorter forecasting horizons. This can also be seen for other Turbines. The new spGWPPT model provides by far the lowest aggregated error measures, suggesting that respecting the Turbines' spatial interaction provides a good share of additional forecasting accuracy. Also, spWPPT does not increase so drastically at increasing forecasting horizons. This suggests that spWPPT could also be used for longer forecasting horizons. Similar results hold true for the other Turbines, as Figure 4 shows.
Table 4 presents sRMSE results for selected forecasting horizons (1 step = 10 minutes, 72 steps = 12 hours, 144 steps = 24 hours, 216 steps = 36 hours). Lowest ("best") values are in bold. In almost all cases, spGWPPT provides the best forecasting accuracy. Furthermore, the Table shows the percentage difference between spGWPPT and the second best model, GWPPT. However, there are cases of significant decrease or insignificant effects, in almost all cases, the accuracy is significantly increased (according to Diebold-Mariano tests). From that we conclude that the newly suggested model provides important enhancements to the field of wind power forecasting.

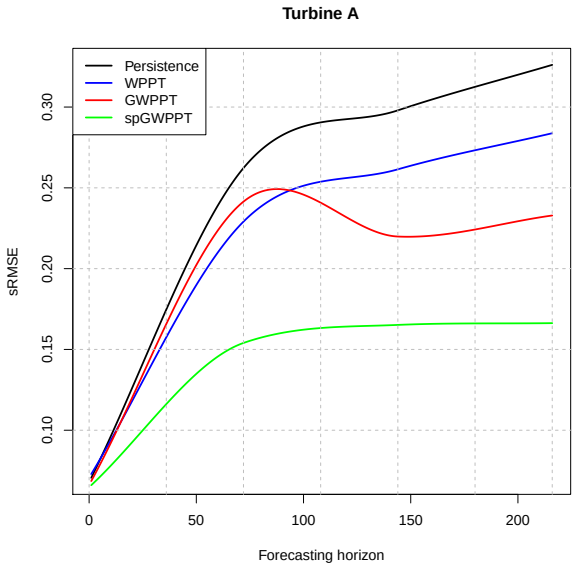

Figure 3. sRMSE for all models and all forecasting horizons, Turbine A, based on 1000 randomly selected observations in the out-of-sample time frame.

	Persistence	WPPT	GWPPT	spGWPPT	GWPPT vs. spGWPPT
Turbine A					
1 Step	0.0705	0.0729	0.0706	**0.0660**	***+7.0%
72 Steps	0.2623	0.2291	0.2427	**0.1540**	***+57.6%
144 Steps	0.2980	0.2615	0.2191	**0.1652**	***+32.6%
216 Steps	0.3261	0.2838	0.2329	**0.1663**	***+40.1%
Turbine B					
1 Step	0.0722	0.0757	**0.0606**	0.0701	***–13.5%
72 Steps	0.2685	0.2238	0.3098	**0.1716**	***+80.5%
144 Steps	0.3030	0.2704	0.2339	**0.1865**	***+25.4%
216 Steps	0.3271	0.2957	0.2381	**0.1881**	***+26.6%
Turbine C					
1 Step	0.0773	0.0800	**0.0606**	0.0636	***–4.7%
72 Steps	0.2720	0.2299	0.1781	**0.1748**	+1.9%
144 Steps	0.3068	0.2784	0.1993	**0.1899**	+4.9%
216 Steps	0.3343	0.3086	0.2028	**0.1905**	+6.5%
Turbine D					
1 Step	0.0767	0.0823	0.0698	**0.0630**	***+10.8%
72 Steps	0.2703	0.2373	0.1767	**0.1685**	+4.9%
144 Steps	0.3026	0.2807	0.1943	**0.1802**	+7.8%
216 Steps	0.3301	0.2992	0.2032	**0.1801**	+12.8%

Table 4. sRMSE results per Turbine and forecasting horizon. ***, ** and * represent significance at 1%, 5%, and 10% level, according to Diebold-Mariano tests. Lowest ("best") values are in bold.

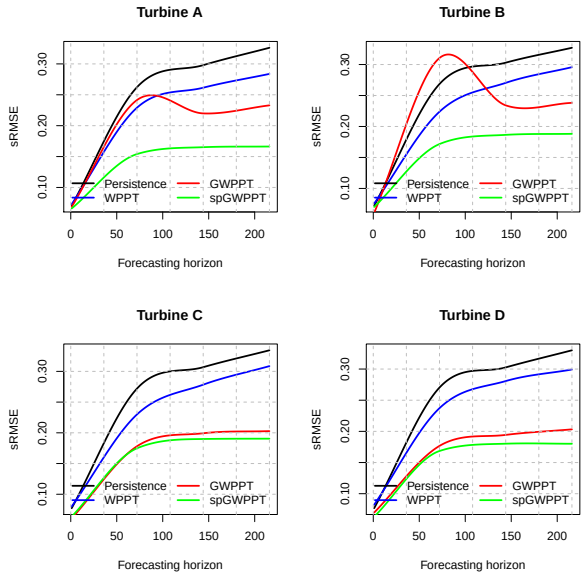

Figure 4. sRMSE for all models and all forecasting horizons, Turbines A to D, based on 1000 randomly selected observations in the out-of-sample time frame.

5 Conclusion

In this article we discuss the impact of the spatial interaction between several turbines located in close proximity, a typical arrangement of wind parks. First, we provide two tests to check for wake effects and their suspected negative influence on power production. Based on that, we introduce a Spatial Lag Model specification for a data set of four turbines. We generalize the GWPPT model and respect both-sided censoring of the data as well as random effects inside the panel data structure. An empirical comparison of forecasting performance shows that the newly proposed model provides significantly increased prediction accuracy compared to current state-of-the-art models.

Appendix

Gauss-Hermite quadrature for approximating the integral in (12):

$$\begin{aligned} L_i = & \frac{1}{\sqrt{\pi}} \sum_{h=1}^{H} \zeta_h \left(\prod_{t=1}^{T_i} \left(\Phi \left(\frac{l - x_{it}^T \beta - \sqrt{2}\sigma_\theta \psi_h}{\sigma_\omega} \right) \right)^{I_{it}^l} \right. \\ & \left(\Phi \left(\frac{x_{it}^T \beta + \sqrt{2}\sigma_\theta \psi_h - u}{\sigma_\omega} \right) \right)^{I_{it}^u} \\ & \left. \left(\frac{1}{\sigma_\omega} \phi \left(\frac{y_{it} - x_{it}^T \beta - \sqrt{2}\sigma_\theta \psi_h}{\sigma_\omega} \right)^{\left(1 - I_{it}^l - I_{it}^u\right)} \right) \right), \end{aligned} \tag{13}$$

where H denotes the number of quadrature points, $\psi_1, \ldots, \psi_H$ are the respective abscissae, and $\zeta_1, \ldots, \zeta_H$ are the weights (see Greene, 2003, p. 693, and Henningsen, 2010).

$$\frac{\partial \log L_i}{\partial \beta_j} = \frac{1}{\sqrt{\pi} L_i} \sum_{h=1}^{H} \zeta_h \left(\left(\prod_{t=1}^{T_i} \left(\Phi \left(\frac{l - x_{it}^T \beta - \sqrt{2}\sigma_\theta \psi_h}{\sigma_\omega} \right) \right)^{I_{it}^l} \right.\right.$$
$$\left(\Phi \left(\frac{x_{it}^T \beta + \sqrt{2}\sigma_\theta \psi_h - u}{\sigma_\omega} \right) \right)^{I_{it}^u} \left(\frac{1}{\sigma_\omega} \phi \left(\frac{y_{it} - x_{it}^T \beta - \sqrt{2}\sigma_\theta \psi_h}{\sigma_\omega} \right) \right)^{\left(1 - I_{it}^l - I_{it}^u\right)} \Bigg)$$
$$\left(\sum_{t=1}^{T_i} \left(- \frac{\phi \left(\frac{l - x_{it}^T \beta - \sqrt{2}\sigma_\theta \psi_h}{\sigma_\omega} \right)}{\Phi \left(\frac{l - x_{it}^T \beta - \sqrt{2}\sigma_\theta \psi_h}{\sigma_\omega} \right)} \frac{x_{ijt}}{\sigma_\omega} \right)^{I_{it}^l} \left(\frac{\phi \left(\frac{x_{it}^T \beta + \sqrt{2}\sigma_\theta \psi_h - u}{\sigma_\omega} \right)}{\Phi \left(\frac{x_{it}^T \beta + \sqrt{2}\sigma_\theta \psi_h - u}{\sigma_\omega} \right)} \frac{x_{ijt}}{\sigma_\omega} \right)^{I_{it}^u} \right.$$
$$\left. \left. \left(- \frac{\phi' \left(\frac{y_{it} - x_{it}^T \beta - \sqrt{2}\sigma_\theta \psi_h}{\sigma_\omega} \right)}{\phi \left(\frac{y_{it} - x_{it}^T \beta - \sqrt{2}\sigma_\theta \psi_h}{\sigma_\omega} \right)} \frac{x_{ijt}}{\sigma_\omega^2} \right)^{\left(1 - I_{it}^l - I_{it}^u\right)} \right) \right) \tag{14}$$

$$\frac{\partial \log L_i}{\partial \log \sigma_\theta} = \frac{\sigma_\theta}{\sqrt{\pi} L_i} \sum_{h=1}^{H} \zeta_h \left(\left(\prod_{t=1}^{T_i} \left(\Phi \left(\frac{l - x_{it}^T \beta - \sqrt{2}\sigma_\theta \psi_h}{\sigma_\omega} \right) \right)^{I_{it}^l} \right.\right.$$
$$\left(\Phi \left(\frac{x_{it}^T \beta + \sqrt{2}\sigma_\theta \psi_h - u}{\sigma_\omega} \right) \right)^{I_{it}^u} \left(\frac{1}{\sigma_\omega} \phi \left(\frac{y_{it} - x_{it}^T \beta - \sqrt{2}\sigma_\theta \psi_h}{\sigma_\omega} \right) \right)^{\left(1 - I_{it}^l - I_{it}^u\right)} \Bigg)$$
$$\left(\sum_{t=1}^{T_i} \left(- \frac{\phi \left(\frac{l - x_{it}^T \beta - \sqrt{2}\sigma_\theta \psi_h}{\sigma_\omega} \right)}{\Phi \left(\frac{l - x_{it}^T \beta - \sqrt{2}\sigma_\theta \psi_h}{\sigma_\omega} \right)} \frac{\sqrt{2}\psi_h}{\sigma_\omega} \right)^{I_{it}^l} \left(\frac{\phi \left(\frac{x_{it}^T \beta + \sqrt{2}\sigma_\theta \psi_h - u}{\sigma_\omega} \right)}{\Phi \left(\frac{x_{it}^T \beta + \sqrt{2}\sigma_\theta \psi_h - u}{\sigma_\omega} \right)} \frac{\sqrt{2}\psi_h}{\sigma_\omega} \right)^{I_{it}^u} \right.$$
$$\left. \left. \left(- \frac{\phi' \left(\frac{y_{it} - x_{it}^T \beta - \sqrt{2}\sigma_\theta \psi_h}{\sigma_\omega} \right)}{\phi \left(\frac{y_{it} - x_{it}^T \beta - \sqrt{2}\sigma_\theta \psi_h}{\sigma_\omega} \right)} \frac{\sqrt{2}\psi_h}{\sigma_\omega^2} \right)^{\left(1 - I_{it}^l - I_{it}^u\right)} \right) \right) \tag{15}$$

$$
\begin{aligned}
\frac{\partial \log L_i}{\partial \log \sigma_\omega} =& \frac{\sigma_\omega}{\sqrt{\pi} L_i} \sum_{h=1}^{H} \zeta_h \left(\left(\prod_{t=1}^{T_i} \left(\Phi \left(\frac{l - x_{it}^T \beta - \sqrt{2}\sigma_\theta \psi_h}{\sigma_\omega} \right) \right)^{I_{it}^l} \right. \right. \\
& \left(\Phi \left(\frac{x_{it}^T \beta + \sqrt{2}\sigma_\theta \psi_h - u}{\sigma_\omega} \right) \right)^{I_{it}^u} \left(\frac{1}{\sigma_\omega} \phi \left(\frac{y_{it} - x_{it}^T \beta - \sqrt{2}\sigma_\theta \psi_h}{\sigma_\omega} \right) \right)^{\left(1 - I_{it}^l - I_{it}^u\right)} \Bigg) \\
& \left(\sum_{t=1}^{T_i} \left(- \frac{\phi \left(\frac{l - x_{it}^T \beta - \sqrt{2}\sigma_\theta \psi_h}{\sigma_\omega} \right)}{\Phi \left(\frac{l - x_{it}^T \beta - \sqrt{2}\sigma_\theta \psi_h}{\sigma_\omega} \right)} \frac{l - x_{it}^T \beta - \sqrt{2}\sigma_\theta \psi_h}{\sigma_\omega^2} \right)^{I_{it}^l} \right. \\
& \left(\frac{\phi \left(\frac{x_{it}^T \beta + \sqrt{2}\sigma_\theta \psi_h - u}{\sigma_\omega} \right)}{\Phi \left(\frac{x_{it}^T \beta + \sqrt{2}\sigma_\theta \psi_h - u}{\sigma_\omega} \right)} \frac{x_{it}^T \beta + \sqrt{2}\sigma_\theta \psi_h - u}{\sigma_\omega^2} \right)^{I_{it}^u} \left(- \frac{1}{\sigma_\omega} \right. \\
& \left. \left. \left. - \frac{\phi' \left(\frac{y_{it} - x_{it}^T \beta - \sqrt{2}\sigma_\theta \psi_h}{\sigma_\omega} \right)}{\phi \left(\frac{y_{it} - x_{it}^T \beta - \sqrt{2}\sigma_\theta \psi_h}{\sigma_\omega} \right)} \frac{y_{it} - x_{it}^T \beta - \sqrt{2}\sigma_\theta \psi_h}{\sigma_\omega^2} \right)^{\left(1 - I_{it}^l - I_{it}^u\right)} \right) \right) \qquad (16)
\end{aligned}
$$

References

Alexiadis, M., Dokopoulos, P., and Sahsamanoglou, H. (1999), Wind Speed and Power Forecasting Based on Spatial Correlation Models, *IEEE Transactions on Energy Conversion*, vol. 14, pp. 836 – 842.

Costa, A., Crespo, A., Navarro, J., Lizcano, G., Madsen, H., and Feitosa, E. (2008), A Review on the Young History of the Wind Power Short Term Prediction, *Renewable and Sustainable Energy Reviews*, 12, pp. 1725–1744.

Croonenbroeck, C. and Dahl, C.M. (2014), Accurate Medium-Term Wind Power Forecasting in a Censored Classification Framework, *Energy*, 73, pp. 221 – 232.

Damousis, I., Alexiadis, M.C., Theocharis, J.B., and Dokopoulos, P.S. (2004), A Fuzzy Model for Wind Speed Prediction and Power Generation in Wind Parks Using Spatial Correlation, *IEEE Transactions on Energy Conversion*, vol. 19, pp. 352 – 361.

Díaz, G., Casielles, P.G., and Coto, J. (2014), Simulation of Spatially Correlated Wind Power in Small Geographic Areas – Sampling Methods and Evaluation, *Electrical Power and Energy Systems*, 63, pp. 513 – 522.

Elhorst, J.P. (2010), Applied Spatial Econometrics: Raising the Bar, *Spatial Economic Analysis*, 5(1), pp. 9 – 28.

Giebel, G., Brownsword, R., Kariniotakis, G., Denhard, M., and Draxl, C. (2011), The State-Of-The-Art in Short-Term Prediction of Wind Power, Tech. rep., ANEMOS.plus, Risø DTU, Wind Energy Division.

Greene, W.H. (2003), *Econometric Analysis*, Prentice Hall.

Han, Y. and Chang, L. (2010), A Study of the Reduction of the Regional Aggregated Wind Power Forecast Error by Spatial Smoothing Effects in the Maritimes Canada, *2nd IEEE International Symposium on Power Electronics for Distributed Generation Systems*, pp. 942 – 947.

Henningsen, A. (2010), Estimating Censored Regression Models in R using the censReg Package, *R package vignettes collection, v0.5 – 2*.

Hering, A.S. and Genton, M.G. (2010), Powering Up With Space-Time Wind Forecasting, *Journal of the American Statistical Assiciation*, 105(489), pp. 92–104.

Kim, S.H., Shin, H.K., Joo, Y.C., and Kim, K.H. (2015), A Study of the Wake Effects on the Wind Characteristics and Fatigue Loads for the Turbines in a Wind Farm, *Renewable Energy*, 74, pp. 536 – 543.

Lei, M., Shiyan, L., Chuanwen, J., Hongling, L., and Zhang, Y. (2009), A Review on the Forecasting of Wind Speed and Generated Power, *Renewable and Sustainable Energy Reviews*, 13, pp. 915–920.

Li, H., Calder, C.A., and Cressie, N. (2007), Beyond Moran's I: Testing for Spatial Dependence Based on the Spatial Autoregressive Model, *Geographical Analysis*, 39(4), pp. 357 – 375.

Nielsen, H.A., Pinson, P., Christiansen, L.E., Nielsen, T.S., Madsen, H., Badger, J., Giebel, G., and Ravn, H.F. (2007), Improvement and Automation of Tools for Short Term Wind Power Forecasting, Tech. rep., Scientific Proceedings of the European Wind Energy Conference & Exhibition, Milan, Italy.

Xie, L., Gu, Y., Zhu, X., and Genton, M.G. (2011), Power System Economic Dispatch with Spatio-Temporal Wind Forecasts, *IEEE Energytech*, pp. 1 – 6.